

## Structural effect of cationic surfactant on heavy metal removal capacity of raw sepiolite

Yasemen Kalpakli\* & Hilal Cansev

Chemical Engineering Department , Yildiz Technical University , Davutpasa Campus, No.

127, Esenler 34210, Istanbul , Turkey

E-mail: yaseminkalpakli@gmail.com

*Received 22 February 2016; accepted 27 April 2017*

Important features like the change of surface properties from hydrophilic to hydrophobic and the change of surface charge from negative to positive, enable the production of organosepiolites from sepiolites, their use in various processes including adsorption of organic pollutants, removal of heavy metal contaminants and water treatment processing.

Organo-clays have been synthesized using Turkey (Sivrihisar/Eskişehir) smectite and the cationic surfactant hexadecyltrimethylammonium bromide (HDTMAB). Moreover, the removal characteristics of  $\text{Cd}^{2+}$ ,  $\text{Cu}^{2+}$  and  $\text{Pb}^{2+}$  ions from aqueous solution by prepared organoclay have been investigated. The changes in the surfaces and structures of the smectites modified with HDTMA surfactant have been characterized using X-ray diffractometry (XRD), Fourier transform infrared spectroscopy (FTIR), Brunauer-Emmett-Teller (BET), Thermogravimetric analysis (TG), Total organic carbon (TOC) and particle size analysis. The XRD patterns show that the intergallery distances of the raw sepiolite increase with the surfactant loading. The FTIR measurements are used to indicate the interactions between the raw sepiolite surface and the HDTMA cations. The BET surface area of the organosepiolites decrease significantly after the modification, due to the coverage of the pores of the raw sepiolite. The thermogravimetric peaks (DTG) in the range between 350–450°C depends on the surfactant loadings and provide the evidence for the formation of the multilayers on the sepiolite surface. The organosepiolite sample that was labeled 1.5h-2CMC, is chosen for next heavy metal adsorption studies.

**Keywords:** X-ray diffraction, Sepiolite, Cationic Surfactant, Total organic carbon

The application of surfactant modified clays as sorbents for heavy metals from the aqueous phase has been active. Most studies have used quaternary ammonium cationic surfactants. With greater loadings, the cationic surfactants are adsorbed on clay surface and intercalate the layers with *both* the ion exchange and hydrophobic bonding<sup>1</sup>.

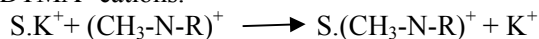
With the Si–OH groups at the edges of the tunnels and exchangeable cations, the surface of the sepiolite can be modified by quaternary ammonium salts, coupling agents and Lewis and Bronsted acids<sup>2</sup>.

Sepiolite is used in a wide range of applications as a result of its high cation exchange capacity, high surface area, and adsorptive/intercalative properties<sup>3,4</sup>. Sepiolite is a fibrous hydrated magnesium silicate and a natural clay mineral with a unit cell formula  $[\text{Si}_{12}\text{Mg}_8\text{O}_{30}(\text{OH})_4(\text{H}_2\text{O})_4\cdot 8\text{H}_2\text{O}]$ . Each block consists of two tetrahedral silica sheets enclosing a central magnesia sheet<sup>5</sup>. The sepiolite structure is constituted by a magnesium octahedral sheet in between 2 layers of silica tetrahedrons which extend as a continuous layer with an inversion of the apical ends every six units<sup>6</sup>. By replacing the inorganic cations ( $\text{Mg}^{2+}$ ) with

organic ones ( $\text{HDTMA}^+$ ), it is possible to convert a naturally hydrophilic property of sepiolite into a hydrophobic and organophilic property<sup>7</sup>. Organoclays are usually synthesized by modifying clay with surfactants via an ion exchange. In this case, most surfactants are intercalated into the clay gallery, while some parts are adsorbed by an external surface<sup>8</sup>. The intercalation of the cationic surfactant not only changes the surface properties from hydrophilic to hydrophobic, but also greatly increases the basal spacing of the layers. This study seeks to show the changes in both the surface and structural properties of the organoclay<sup>3</sup>.

The CMC value is the important point for the intercalation of the surfactant molecules in the modification process. The CMC value of surfactant used in these experiments has been obtained by research in the literature<sup>9,4</sup>. In the aqueous solution surfactant molecules form micelles if the concentration exceeds the critical micelle concentration (CMC)<sup>10</sup>. When the surfactant concentration was less than the CMC,  $[\text{HDTMA}]/\text{CMC} < 1$ , the surfactant molecules were ionized into individual cations and anions in the sepiolite-surfactant suspensions. The Ion exchange

occurs in the interlayer gallery between  $Mg^{2+}$  and  $HDTMA^+$  cations.



S: Sepiolite

$K^+$ : Exchangeable inorganic cations

R: Alkyl group

When the concentration was above the CMC,  $[HDTMA]/CMC > 1$ , the surfactant micelles and individual ions coexisted in the solution. Since the micelles were much more positively charged than the HDTMA cations, they had a greater affinity to the negatively charged sepiolite surface. The intercalation of the excess surfactant cations takes place with the micelles adsorption<sup>4,11</sup>.

(1)  $[HDTMA] < CMC$

The surfactant cations intercalated into the interlayer spaces through the cation exchange, and they adhered to the surface through via electrostatic interaction.

(2)  $[HDTMA] = CMC$

The surfactant molecules physically adsorbed into the external surface of the particles

(3)  $[HDTMA] > CMC$

The surfactant molecules located within the interlayer spaces<sup>12</sup>.

The aim of this paper is to study the modification of raw sepiolite from Sivrihisar/Eskişehir by HDTMA-Br (hexadecyltrimethylammonium bromide), which is a cationic surfactant with different surfactant concentrations (1CMC and 2CMC) and different contact times (1,1.5,2,2.5,3 h). The Raw sepiolite and organosepiolite samples were characterized by XRD, FTIR, BET, TG (thermal analysis) and TOC and particle size analysis techniques.

## Experimental Section

### Materials

The raw sepiolite used in this study was from Sivrihisar/Eskişehir, in Turkey. The sample was ground and sieved with a 65  $\mu m$  sieve. The cation exchange capacity (CEC) determined by the methylene blue method was 21.39 meq/100 g. The surfactant used was the hexadecyltrimethylammonium bromide labeled HDTMA-Br ( $CH_3(CH_2)_{15}(CH_3)_3-N^+Br^-$ ). It was obtained from Merck. Its critical micelle concentration (CMC) was 0.9 mmol/L<sup>13,14</sup>.

### Preparation of organosepiolite

The organosepiolite (HDTMA-sepiolite) was synthesized by using the HDTMA-Br, and was

obtained as a result of ion-exchange reactions. The natural sepiolite was modified in respect to the surfactant critical micelle concentration (CMC). The amount of HDTMA-Br was equal to, 1 or twice, the critical micelle concentration (CMC) of the surfactant. The HDTMA-Br was dissolved in 100 mL of distilled water at 80°C with quantities of 1 CMC and 2 CMC<sup>15</sup>. 5 g of sepiolite samples were dispersed into the 50 mL distilled water by magnetic stirring at 80°C for 1 h, at 400 rpm. The natural sepiolites were mixed with the HDTMA solutions, and the organically modifying time was set at 0.5, 1, 1.5, 2, 2.5, 3 h using a magnetic stirrer at 1200 rpm<sup>16</sup>. The suspensions were filtered through a filter paper. The prepared organo-sepiolites were washed with distilled water several times until free of  $Br^-$ <sup>15-17</sup>. The organosepiolites were dried in an oven at 100°C for 24 h. They were sieved with a 100  $\mu m$  sieve.

### Characterization methods

The X-ray powder diffraction measurements of the organosepiolite samples were carried out using a Bruker AXS diffractometer. The XRD patterns of the raw sepiolite and organosepiolite samples were also recorded between 3 and 80° (2 $\theta$ ) at a step size of 0.02°. The basal spacing of the silicate layer (d) was calculated using the Bragg's equation:  $d = \lambda / (2 \sin \theta)$ . The fourier transform infrared (FTIR) analysis of the natural sepiolite and the organosepiolite samples were performed with a Perkin Elmer Universal ATR model infrared spectrophotometer. The Spectra were recorded over a spectral range between 4000 and 650  $cm^{-1}$  with 4  $cm^{-1}$ . The BET surface areas of the raw sepiolite and organosepiolites were determined from the  $N_2$  adsorption isotherm with a surface area analyzer (A Quantachrome Autosorb Automated Gas Sorption System). The thermal characterization of the organosepiolites was obtained using a Exstar 6000 TG/DTA 6300 Series in the temperature range of 25-1050°C at a heating rate of 10°C  $min^{-1}$ , under a nitrogen flow. The amounts of organic substances were, by total organic carbon (TOC) determined with a A Hach Lange IL 550 TOC-TN. The particle size of the raw sepiolite and organosepiolites was determined by a Malvern Mastersizer 2000 model.

## Results and Discussion

### XRD analysis (X-ray diffraction analysis)

The characteristic diffraction peak of the natural sepiolite was found at  $2\theta = 7.3^\circ$  (110) given in Fig. 1. The X-ray diffraction (XRD) analysis, together with

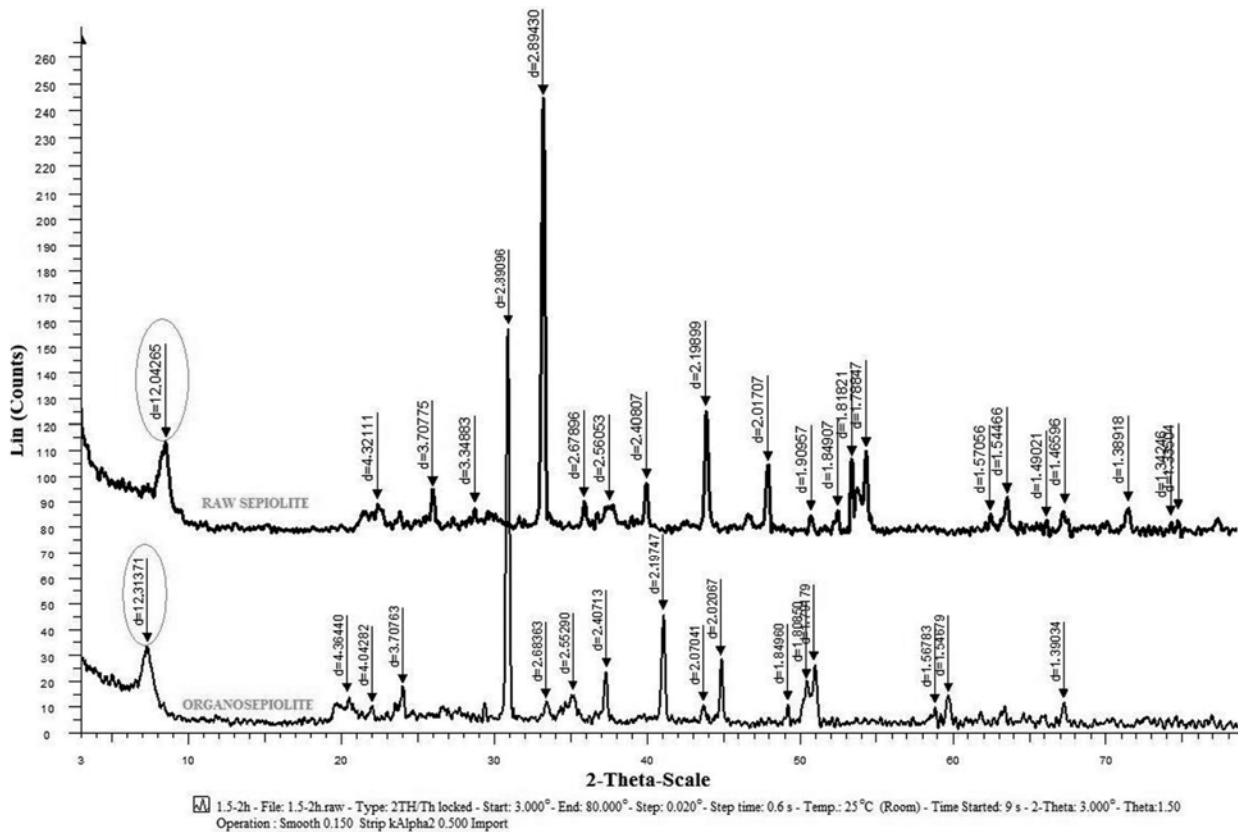


Fig. 1 — XRD spectra of (a) raw sepiolite and (b) the most qualified organosepiolite sample

 Table 1 — Basal spacing  $d(001)$  ( $\text{\AA}$ ) of raw sepiolite and organosepiolite samples

Samples	$d_{001}(\text{\AA})$	
Raw sepiolite	12.04	
HDTMA-sepiolite	1CMC	2CMC
1 h	12.19	12.2
1.5 h	12.3	12.31
2 h	12.21	12.3
2.5 h	12.20	12.24
3 h	12.18	12.20

the chemical analysis (XRF) of the natural sepiolite (30.70%  $\text{SiO}_2$ , 18.25%  $\text{CaO}$ , 17.95%  $\text{MgO}$ ) indicated that both sepiolite and dolomite are the major components along with the trace of  $\text{Al}_2\text{O}_3$  (4.20%) and  $\text{Fe}_2\text{O}_3$  (1.01%) in the form of impurities and loss of ignition (27.75 %).

Table 1 includes  $d(001)$  values of the organosepiolites for the comparison purposes with raw sepiolite. The basal spacings are expanded as expected depending on the surfactant concentrations<sup>15</sup>.

While the basal spacing of the raw sepiolite is 12.04  $\text{\AA}$ , it increased up to 12.31  $\text{\AA}$  in the sample of 1.5 h-2CMC (Table 1). These results confirm that the expansion in the basal spacing of the natural sepiolite

was due to its modification. The surfactants (HDTMA) were both located on the surface and entered into the interlayer spaces of the sepiolite<sup>18</sup>. The intergallery distance of the sepiolite increases with the increase of the organically modified time, but after a while, it begins to decrease due to leaving the weak surfactant cations back to suspension with the effect of the centrifugal force<sup>19</sup>.

#### TOC analysis

The resulting TOC content of the organosepiolites was measured. The adsorbed amounts of the cationic surfactant (HDTMA) on the sepiolite were determined as %CEC. The cation exchange capacity (CEC) also increases with the increasing contact time. The CEC values of the 2CMC samples were greater than the 1CMC due to an increase in concentration of the surfactant (Table 2).

#### BET analysis

The surface areas of the raw sepiolite and organosepiolite samples were determined with the BET method. Table 3 includes the BET surface areas of the raw sepiolite and organosepiolites. Through the

Table 2 — CEC (%) value of organosepiolite samples

	1 CMC					2 CMC				
	1 h	1.5 h	2 h	2.5 h	3 h	1 h	1.5 h	2 h	2.5 h	3 h
100 mL, initial solution, mg/L					410.30					
100 mL, concentration of liquid phase, mg/L	19.75	18.81	16.61	10.88	7.74	19.18	10.89	10.64	8.15	7.24
Adsorbed amount of alkyl ammonium salt in 50 mL, mg/5 g sepiolite, mg/L	390.55	391.49	393.69	399.42	402.56	391.12	399.41	399.66	402.15	403.06
% CEC	95.18	95.41	95.95	97.34	98.11	95.32	97.34	97.40	98.01	98.23

Table 3 — Surface areas of raw sepiolite and organosepiolites

Samples	Surface area (m <sup>2</sup> /g)	
	1 CMC	2 CMC
Raw sepiolite	114.90	114.90
1 h	98.585	84.914
1.5 h	93.582	84.341
2 h	93.082	82.198
2.5 h	90.456	79.257
3 h	86.252	78.238

intercalation of the HDTMA cations, the interparticle pores were covered and the interlamellar spaces were blocked leading to the inhibition of the passage of N<sub>2</sub> molecules. The BET surface area significantly decreased when the raw sepiolite was modified with a surfactant due to the coverage of the pores of the sepiolite<sup>18,5</sup>.

#### FTIR analysis

The FTIR spectra of the raw sepiolite and organosepiolites are shown in Fig. 2. The band at 3564.03 cm<sup>-1</sup> that corresponds to the stretching ( $\nu$ OH) vibrations of the hydroxyl groups (belonging to Mg<sub>3</sub>OH) attached to the octahedral Mg ions located in the interior blocks of raw the sepiolite and organosepiolites<sup>20</sup>. The band at 1451.98 cm<sup>-1</sup> developed due to the hydroxyl bending vibration, which again reflects the presence of bound water<sup>21</sup>. The Si-O coordination bands at 1015.20 cm<sup>-1</sup> represent the stretching of Si-O in Si-O-Si groups of the tetrahedral sheet<sup>20</sup>. The strong bands at 879.73 cm<sup>-1</sup> and 729.21 cm<sup>-1</sup> indicate that the most prevalent carbonate present is dolomite<sup>22</sup>. A pair of strong band at 2916.33 and 2849.02 cm<sup>-1</sup> was observed, and only the organosepiolite could be assigned to the symmetric and asymmetric stretching vibrations of the methylene group ( $\nu_{\text{CH}_2}$ )<sup>23,7,24,25</sup>. The variations observed in the FTIR spectra of the sepiolite interacted with the HDTMA cations which indicate the interaction between the sepiolite particles and the HDTMA molecules<sup>26</sup>.

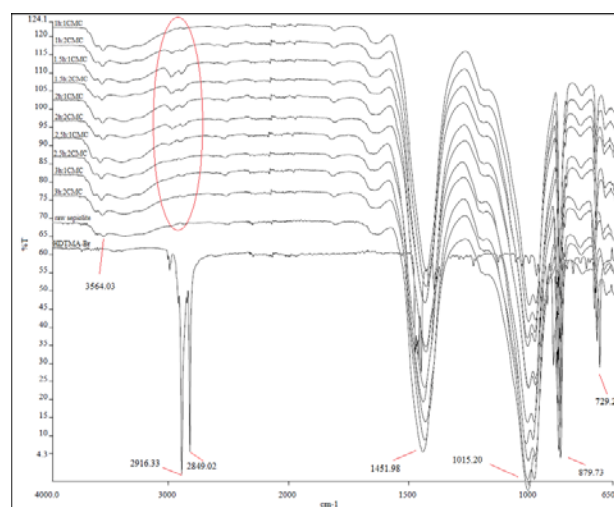


Fig. 2 — FTIR spectra of raw sepiolite and organosepiolite samples

#### Particle size analysis

The particle size values of the raw sepiolite and organosepiolites are presented in Table 4. The analysis of the raw and organosepiolites showed that they contain more coarse particles than the raw sepiolite<sup>27</sup>. The organic cation (HDTMA<sup>+</sup>) replaced the inorganic cation (Mg<sup>+2</sup>), and adhered to the surface of the sepiolite which is stronger than the inorganic cation. The particle size increased due to the fact that more unit layers are kept together<sup>28</sup>. The particle sizes of the organosepiolites increased with the increasing surfactant concentration. However, since the contact time was over 1.5 h, the particle sizes started to decrease regularly.

#### Thermogravimetric analysis of the organosepiolite

The thermal decomposition spectra of the organosepiolite samples were recorded by the TG/DTG/DTA technique. Both Table 5 and Fig. 3 show the DTG results of the raw sepiolite and

Table 4 — The particle size distributions of raw sepiolite and organosepiolites

	Sample	d (0.1) $\mu\text{m}$	d (0.5) $\mu\text{m}$	d (0.9) $\mu\text{m}$
1CMC	Raw sepiolite	1.532	31.732	112.094
	1 h	3.734	38.144	101.772
	1.5 h	5.339	43.361	103.956
	2 h	4.229	41.012	101.515
	2.5 h	3.404	36.526	98.706
	3 h	3.076	34.145	93.746
2CMC	1 h	4.391	40.666	103.438
	1.5 h	5.884	47.361	109.952
	2 h	4.762	43.184	105.515
	2.5 h	4.462	39.391	101.468
	3 h	3.179	37.333	99.611

Table 5 — Mass loss of raw sepiolite and organosepiolite samples

Sample	1. step		2. step		3. step	
	T ( $^{\circ}\text{C}$ )	Mass loss (%)	T ( $^{\circ}\text{C}$ )	Mass loss(%)	T ( $^{\circ}\text{C}$ )	Mass loss (%)
Raw sepiolite	26-142	4.6	219-365	0.9	460-779	25
1h:1 CMC	30-116	3.7	222-355	0.9	522-775	25
1.5h:1 CMC	29-135	3.7	225-358	1	527-796	24.4
2h:1 CMC	22-127	4.1	239-356	0.8	520-781	24.3
2.5h:1 CMC	28-113	4.7	231-326	0.8	523-769	24.5
3h:1 CMC	33-139	4.3	251-364	1.1	505-798	25.2
1h:2 CMC	25-132	3.3	337-461	1.6	535-785	24.2
1.5h:2 CMC	28-129	3.2	329-485	1.9	526-729	24.5
2h:2 CMC	32-146	3.8	351-468	1.7	537-797	24.1
2.5h:2 CMC	27-131	4.2	351-484	0.9	484-783	24.9
3h:2 CMC	24-134	4	337-455	1.5	455-810	25

organosepiolite samples. In the first step, at 0-150 $^{\circ}\text{C}$ , the sepiolite undergoes some weight loss due to the zeolitic water<sup>6</sup>. After the modification of the sepiolite with the surfactant, the intensities of the DTG peaks decreased due to the removal of some of the water between the sepiolite layers<sup>18</sup>. The removal of the octahedral cations (e.g.  $\text{Al}^{3+}$ ,  $\text{Fe}^{3+}$ ,  $\text{Mg}^{2+}$ ) and the hydroxyls, results in the formation of the Lewis and Bronsted centers, and decreases the thermal stability of the sepiolite<sup>8</sup>. The peak intensity at 250 $^{\circ}\text{C}$  decreased in the organosepiolite samples. This was associated with the surfactant adsorbed into the external surfaces of the clay<sup>12</sup>. However, when the surfactant amount was increased during the modification, the peak between 350-450 $^{\circ}\text{C}$  became more apparent. The DTG peaks shown in Fig. 2 at 350-450 $^{\circ}\text{C}$ , correspond to the decomposition of the HDTMA cations between the sepiolite sheets<sup>18</sup>.

When the concentration of the surfactant is relatively low, the organic cations ion exchange with the  $\text{Mg}^{2+}$  ions, and mainly adhere to the surface sites via the electrostatic interactions (lower HDTMA loading). With the increase in the concentration of

the surfactant, some of the surfactant molecules adhere to the surface of the other adsorbed surfactant cations through van der Waals forces (higher HDTMA loading)<sup>29,3</sup>. The strong electrostatic interaction was between the negative charged sepiolite surface and the positively charged head group of the alkylammonium cation ( $\text{HDMTA}^{+}$ ). The sepiolite surface is hydrophilic and hydrocarbon chains of alkylammonium and the cation are hydrophobic<sup>15</sup>. With the increase of the surfactant amount, the surfactant molecules located within the interlayer spaces increase. Thus, the surface of the organosepiolite becomes hydrophobic. The DTG peaks corresponding to the oxidation process became broader with the increasing amount of adsorbed surfactant<sup>9</sup>. There is an expansion in Fig. 3 between 350-500 $^{\circ}\text{C}$ , compared with samples of raw sepiolite.

#### Influence of organic modification on the heavy metal adsorption properties of composites

In order to determine the adsorption capacity of the natural sepiolite and organo-sepiolite, they were kept in contact with 50 mL of Cd(II), Cu(II) and Pb(II) heavy metals solution of various concentrations at an

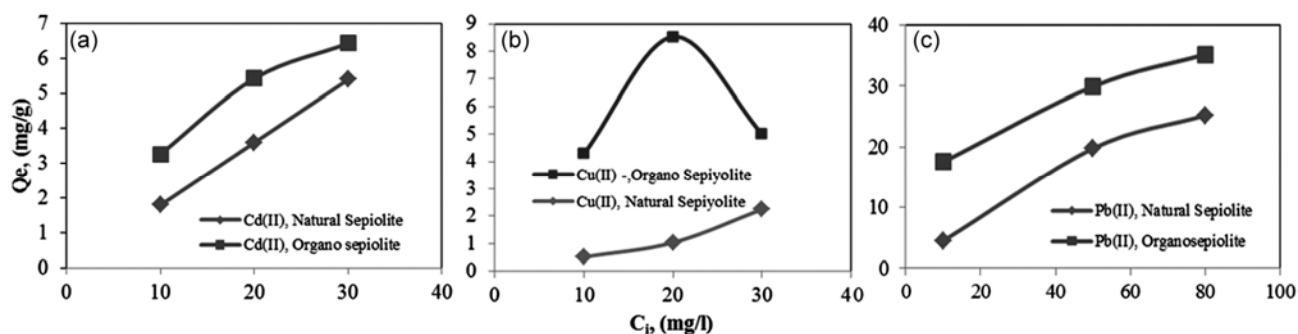


Fig.4 — Adsorption capacities of natural sepiolite and organosepiolite for a) Cd(II), b) Cu(II), c) Pb(II)

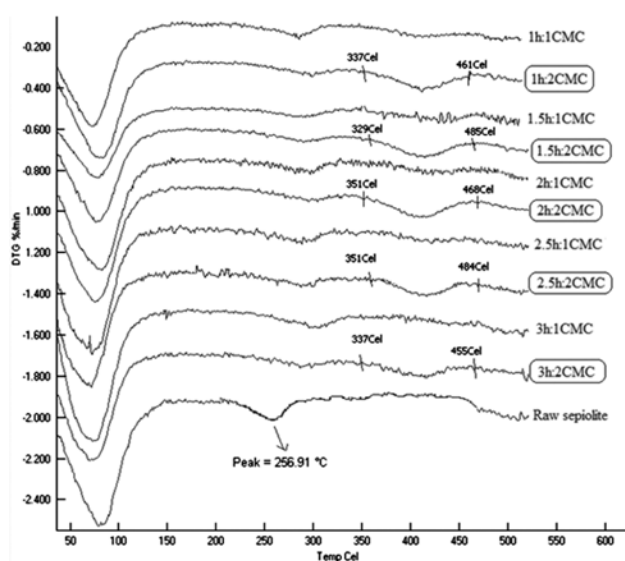


Fig. 3 — Differential thermal analysis patterns of raw and organosepiolite samples

equilibrium time to allow for the attainment of the equilibrium at constant temperature of 20°C.

The maximum sorption capacities corresponding to the natural sepiolite and organo sepiolite with Cd(II), Cu(II) and Pb(II) ions respectively are shown in Fig. 3.

Determining that when using (HDTMA-Br) as an modification agent the capacity and selectivity of sepiolite may improve as adsorbents.

The adsorption capacity for Cu(II) and Cd(II) on the organo sepiolite were obtained as 8.52 mg/g and 5.43 mg/gr for 20 mg/L initial concentration ( $C_i$ , mg/L), respectively. As can be seen, after the surface modification, the sorption capacities increased significantly.

As shown in Fig. 3c, the organo sepiolite samples demonstrate a very high affinity for Pb(II) ion.

When using modified sepiolite as an adsorbent, the adsorption capacity of Pb(II) increased more than the Cu(II) and Cd (II) capacities compared to the natural

sepiolite. The adsorption capacity for the Pb(II) on the organo sepiolite was obtained with 35.14 mg/g for the 80 mg/L initial concentration ( $C_i$ , mg/L). Consequently, it can be seen that there is a selective adsorption of lead by the organosepiolite.

## Conclusion

1) The organosepiolite samples by using different surfactant concentration and different contact times have been characterized using XRD, FTIR, TG/DTG (thermal analysis), BET, TOC, and particle size analysis. According to the result of all the analysis, the most qualified sample is the 2CMC-1.5 h in the adsorption studies.

2) The XRD analysis indicate that the conformation of the HDTMA cation within the gallery spacing of the layered silicate strongly depends on the quantity of the surfactant loaded. When all the samples are observed, there is a difference between the basal space of the 1CMC and 2CMC samples. In fact, the micelle intercalation/adsorption of the cationic surfactant is previously observed at above CMC on sepiolite<sup>4</sup>.

The basal spacing increase up to 12.31 Å in the sample of 1.5h -2CMC. When the surfactant concentration is equal to CMC, the surfactant molecules physically adsorb on the external surface of the particles. In addition, if the surfactant concentration is above CMC, the surfactant molecules locate themselves within the interlayer spaces<sup>12</sup>. The basal space values in Table 1 are evidence of this modification.

3) When the FTIR spectra of the raw sepiolite and organosepiolite samples are compared with the spectra of the sepiolite interacted with the surfactant cations, some displacements are observed in the peak positions<sup>26</sup>. One of the most observable variations obtained is in the FTIR spectra of 2CMC-1.5 h sample in the 2916.33 and 2849.02  $\text{cm}^{-1}$ . These variations in the FTIR spectra of organosepiolite

samples indicate the surfactant molecules located within the interlayer spaces<sup>12</sup>.

4) CEC (cation exchange capacity) generally increases with the increasing contact time and the decreasing particle size of the exchanger. Table 2 and Table 4 support these views.

5) When the concentration of the surfactant increased, expansions are observed in the DTG peaks at 350-500°C. These expansions are more explicit in the DTG peaks of 2CMC samples. These displacements are also further evidence of the modification process.

6) While the organically modifying time continues to increase, the surface areas of organosepiolites decrease<sup>27</sup>. The surface areas of organosepiolites decreased depending on increasing surfactant concentration.

7) As a result of the modification of the sepiolite organo course, the ion adsorption capacity of the lead, copper and cadmium are found to increase.

## References

- Chen H, Zhou W, Zhu K, Zhan H & Jiang M, *Sci Total Environ*, 326 (2004) 217.
- Hongxianga C, Danlina Z, Xiaoqinb X, Maoshengc Z, Changmei K & Yanjun L, *Mater Sci Eng A*, 528 (2011) 1656.
- Zhou Q, Frost R L, He H & Xi Y, *J Colloid Interface Sci*, 307 (2007) 50.
- Feng X, Hu G, Meng X, Ding Y, Zhang S & Yang M, *Appl Clay Sci*, 45 (2009) 239.
- Özcan A S & Gök Ö, *J Mol Spectrosc*, 1007 (2012) 36
- Tartaglione G, Tabuani D & Camino G, *Microporous Mesoporous Mater*, 107 (2008) 161.
- Rožic D M, Šipušić I, Sekovanić L, Miljanić S, Čurković L & Hrenović J, *J Colloid Interface Sci*, 331 (2009) 295.
- Shen W, He H, Zhu J, Yuan P, Ma Y & Liang X, *Chin Sci Bull*, 54/2 (2009) 265.
- Lemic J, Tomašević-Canović M, Djurić M & Stanić T, *J Colloid Interface Sci*, 292 (2005) 11.
- Li Z & Bowman R S, *Environ Sci Technol*, 31 (1997) 2407.
- Zhao Z, Tang T, Qin Y & Huang B, *Langmuir*, 19 (2003) 9260.
- Zidelkheir B & Abdelgoad M, *J Therm Anal Calorim*, 94/1 (2008) 181.
- Li Z, *Microporous Mesoporous Mater*, 116 (1-3) (2008) 473.
- He H, Frost R L, Bostrom T, Yuan P, Duong L, Yang D, Xi Y & Klopogge J T, *Appl Clay Sci*, 31 (2006) 262.
- Xiao W, Zhan M & Li Z, *Mater Des*, 24 (2003) 455.
- Yang L, Jiang L, Zhou Z, Chen Y & Wang X, *Chemos*, 48 (2002) 461.
- Erdem B, Özcan A S & Özcan A, *Surf Interface Anal*, 42 (2010) 1351.
- Tils H M G C & Tels M, *Int J Miner Process*, 36 (3-4) (1992) 201.
- Özcan A, Öncü E M & Özcan A S, *J Hazard Mater*, 129 (2006) 244.
- Alkan M, Tekin G & Namli H, *Microporous Mesoporous Mater*, 84 (2005) 75.
- Snyder R W & Painter P C, *Am Chem Soc*, (1982) 122.
- Özcan A S & Özcan A, *J Hazard Mater B*, 125 (2005) 252.
- Lee S Y & Kim S J, *Appl Clay Sci*, 22 (2002) 55.
- Hongping H, Frost L R & Jianxi Z, *Spectrochim Acta Part A*, 60 (2004) 2853.
- Tunç S, Duman O & Çetinkaya A, *Colloids Surf A: Physicochem Eng Asp*, 377 (2011) 123.
- Yıldız N, Gönülşen R, Koyuncu H & Çalimli A, *Colloids Surf A: Physicochem Eng Asp*, 260 (2005) 87.
- Yıldız N, Köroğlu F, Çalimli A. Eskişehir Osmangazi Üniversitesi Müh.Mim.Fak.Dergisi, (2006) C.XIX-2.
- Gładysz-Plaska A, Majdan M, Pikus S & Sternik D, *Chem Eng J*, 179 (2012) 140.